

Mechanochemical synthesis of organoselenium compounds

Received: 18 May 2023

Accepted: 9 January 2024

Published online: 26 January 2024



Shanshan Chen¹, Chunying Fan¹, Zijian Xu², Mengyao Pei¹, Jiemin Wang¹, Jiye Zhang¹, Yilei Zhang³, Jiyu Li⁴, Junliang Lu⁴, Cheng Peng¹ & Xiaofeng Wei¹

We disclose herein a strategy for the rapid synthesis of versatile organoselenium compounds under mild conditions. In this work, magnesium-based selenium nucleophiles are formed in situ from easily available organic halides, magnesium metal, and elemental selenium via mechanical stimulation. This process occurs under liquid-assisted grinding (LAG) conditions, requires no complicated pre-activation procedures, and operates broadly across a diverse range of aryl, heteroaryl, and alkyl substrates. In this work, symmetrical diselenides are efficiently obtained after work-up in the air, while one-pot nucleophilic addition reactions with various electrophiles allow the comprehensive synthesis of unsymmetrical monoselenides with high functional group tolerance. Notably, the method is applied to regioselective selenylation reactions of diiodoarenes and polyaromatic aryl halides that are difficult to operate via solution approaches. Besides selenium, elemental sulfur and tellurium are also competent in this process, which showcases the potential of the methodology for the facile synthesis of organochalcogen compounds.

As an essential trace element for human beings, selenium manifests a wide range of physiological processes through incorporation into over 25 selenoproteins as selenocysteine¹. The selenium-containing compounds are also prevalent in pharmaceutical libraries^{2–6}, catalyst scaffolds^{7–18}, and material building blocks^{19,20} (Fig. 1a). These important applications have triggered the development of robust, concise, and environmentally friendly methods for their synthesis to access new chemical spaces. Whilst many synthetic methods including metal-catalyzed (Ni, Cu, Pd, Fe, Co, In, etc.) cross-coupling reactions, metal-free oxidative coupling reactions, as well as photochemical and electrochemical reactions have been developed for the synthesis of organoselenium compounds using preformed activated selenium reagents^{21–36}, direct utilization of elemental selenium in the synthesis is a more attractive strategy due to elemental selenium's low price, commercial availability, storage stability, odourlessness, and ease of handling. Nevertheless, the inert chemical property, low solubility in

organic solvent, and tendency to form transition-metal selenium clusters make direct use of selenium powder for efficient synthesis challenging (Fig. 1b)³⁷. To date, the majority of these methods require large excess of polar solvents, long reaction time, and harsh conditions. In contrast with traditional solvent-based strategies, mechanochemistry allows efficient energy dispersion and mass transportation under solid-state condition and therefore provides an alternative strategy for green and sustainable synthesis^{38–47}. Recently, the strategy has been applied to facilitate the oxidative addition of zero valent metals (such as Mg, Mn, Zn, Ca, etc) to organic halides, generating organometallic species for diverse nucleophilic transformations^{48–60}. For instance, Ito, Kubota⁶⁰, and Bolm⁶¹ groups independently demonstrated elegant examples of producing versatile Grignard reagents using mechanochemical strategy. Remarkably, in the work of Ito and Kubota⁶⁰, no degradation of air-sensitive Grignard reagents was observed even when the milling jar was briefly

¹School of Pharmacy, Xi'an Jiaotong University, No. 76, Yanta West Road, Xi'an 710061, China. ²Shanghai Synchrotron Radiation Facility, Shanghai Advanced Research Institute, Chinese Academy of Sciences, Shanghai 201204, China. ³Department of Biochemistry and Molecular Biology, School of Basic Medical Sciences, Xi'an Jiaotong University Health Science Center, Xi'an, Yanta, China. ⁴Xi'an Aisiyi Health Industry Co., Ltd, Xi'an 710075, China.

✉ e-mail: pcheng@xjtu.edu.cn; xiaofeng.wei@xjtu.edu.cn

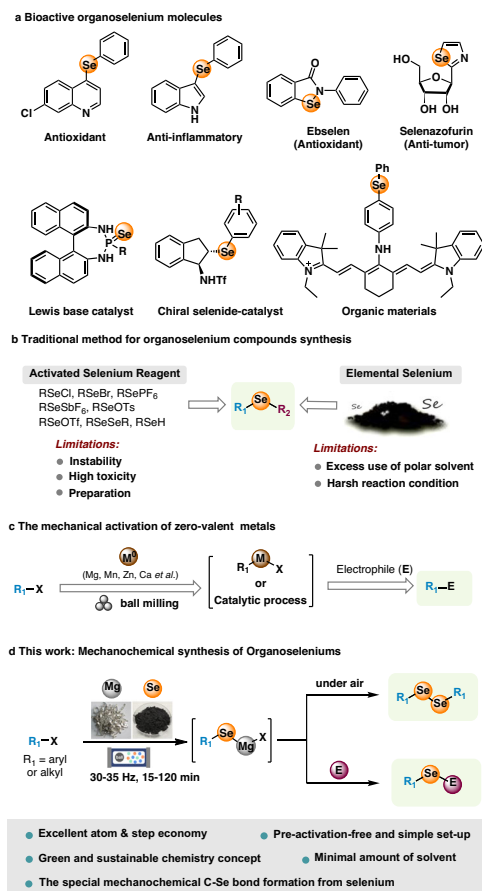


Fig. 1 | Synthesis of organoselenium compounds. **a** Functional organoselenium molecules; **b** Traditional method for organoselenium compounds synthesis; **c** The mechanical activation of zero-valent metals; **d** Mechanochemical route.

exposed to the air before adding an electrophile, highlighting the method's robustness.

In this work, we present a mechanochemical method for synthesizing organoselenium compounds which involves the in situ generation of magnesium-based selenium species through the straightforward process of mixing and grinding organic halides, magnesium, and elemental selenium. Notably, these species exhibit extreme sensitivity to both oxygen and water, leading to their complete conversion into symmetrical diselenides during the work-up procedure. Additionally, employing a one-pot process for the addition of electrophiles enables efficient synthesis of unsymmetrical monoselenides, which proceeds smoothly even in the presence of air. (Fig. 1d). We also achieve the successful preparation of magnesium-based organoselenium reagents from polyaromatic aryl halides and diiodoarenes. Notably, it's important to highlight that converting such substrates into organochalcogenides poses challenges when employing conventional solution-based methods. Near edge X-ray absorption fine structure (NEXAFS) spectroscopy is employed to analyze the generation of the magnesium-based organoselenium nucleophiles under mechanochemical conditions. The method can be extended to the straightforward synthesis of organic sulfur and tellurium compounds, suggesting its potential to serve as a highly practically foundation for the comprehensive synthesis of organochalcogen compounds.

Results

As a proof of concept, we chose iodobenzene (**1a**) as a model substrate to be added to a 1.5 mL stainless-steel milling jar loaded with commercially available magnesium turnings (1.0 equiv relative to **1a**),

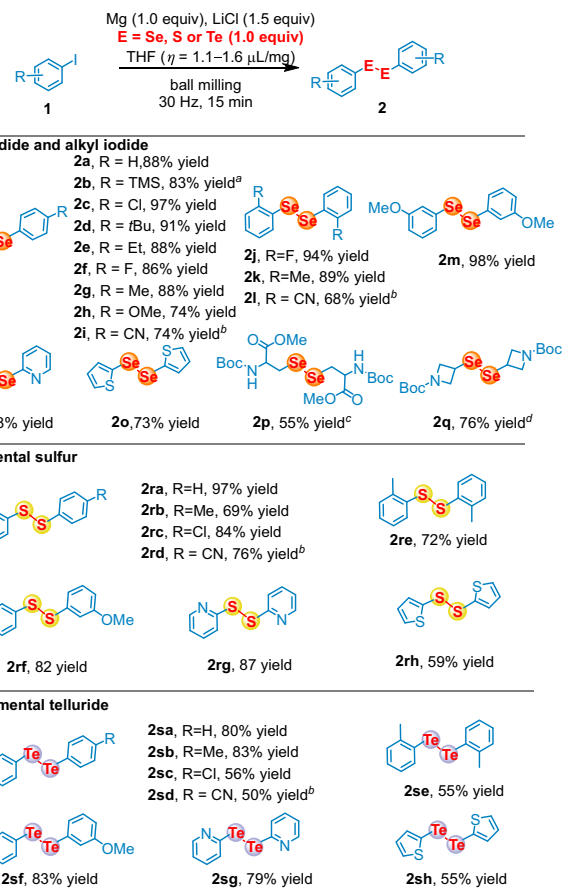
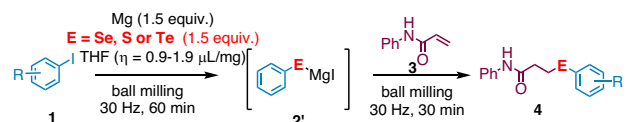
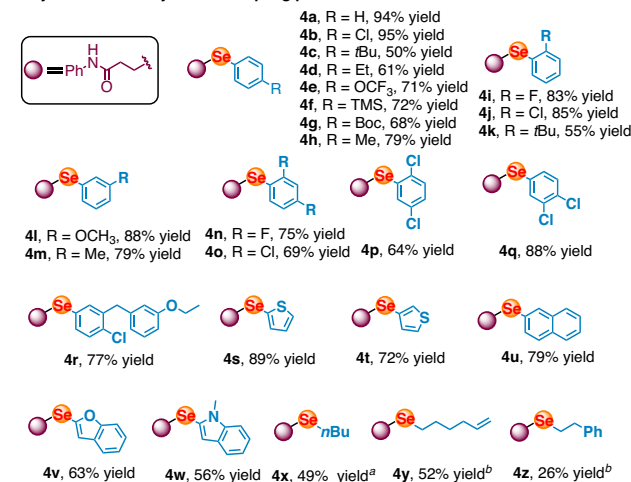
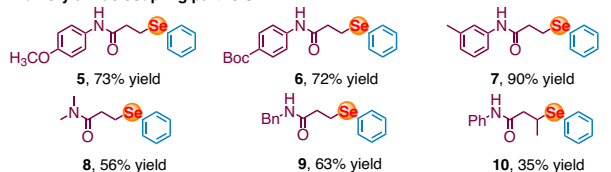
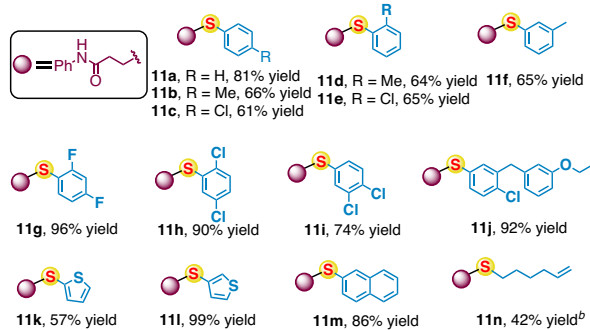
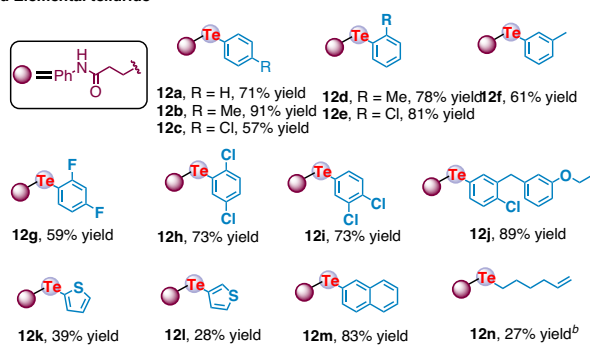


Fig. 2 | Substrate scope for the synthesis of symmetrical dichalcogenides. **a** Aryl iodide and alkyl iodide; **b** Elemental sulfur; **c** Elemental telluride. Reaction conditions: a stainless-steel milling jar (1.5 mL) and a stainless-steel ball (6 mm) were used; isolated yields; $\eta = V$ (liquid; μL) / m (reagents; mg). For details, see the Supplementary Information Condition A; ^a**1b** = 4-TMS-PhBr; ^b60 min, 35 Hz, Mg (1.5 equiv); ^c120 min, 35 Hz, Mg (0.5 equiv). For details, see the Supplementary Information Condition C; ^d30 min.

selenium powder (1.0 equiv relative to **1a**), LiCl (1.5 equiv relative to **1a**), THF ($\eta = 1.4 \mu L/mg$), and one stainless-steel balls (diameter: 6 mm) in argon glovebox (For detailed screening of reaction parameters, see the Supplementary Information, Supplementary Table 2). The reaction was conducted using Retch MM400, while Retch MM500 was used in the case of higher vibration frequency (35 Hz). The reaction was monitored and the starting material was completely consumed within 15 min. To our surprise, instead of getting benzeneselenol, which was the predominant product in solvent-based activation of elemental selenium using Grignard reagents⁶²⁻⁶⁴, diphenyl diselenide was obtained in 88% yield (Fig. 2a). Analysis of crude NMR showed only approximately 5% benzeneselenol was generated, while potential side products such as biphenyl and diphenylselenide were not observed. The high chemoselectivity for diselenide showed the advantage of our strategy. Up to date, preparation of diselenide from elemental selenium generally requires a transition metal catalyst, harsh reaction conditions, and long reaction time⁶⁵⁻⁶⁸, indicating our approach provides a solution for their facile synthesis.

Having established the optimal conditions, we next examined the scope of the reaction. Products were obtained in high yield for aryl iodides possessing electron-donating groups, halogen, and sterically hindered substituents at all *para*-, *ortho*-, and *meta*- positions (**2a**, **2c-2h**, **2j-2k**, **2m**, 74-98%). Aryl bromide (**1b**) also performed well under the optimized condition (**2b**, 83%). Heteroaryl iodides (**1n** and **1o**) were also competent under the standard reaction as the corresponding

**a Aryl iodide and alkyl iodide coupling partners****b Acrylamide coupling partners****c Elemental sulfur****d Elemental telluride**

products were isolated in satisfying results (**2n** and **2o**, 88% and 73%). Substrates with relatively strong electron-withdrawing nitrile substitution at *ortho*- or *para*- position (**1l** and **1i**) showed decreased reactivity while increasing the loading of magnesium as well as the vibration frequency significantly improved the yields (**2l** and **2i**, 68% and 74%). It is worth noting that both elemental sulfur and tellurium were also applicable, providing symmetrical disulfides and ditellurides

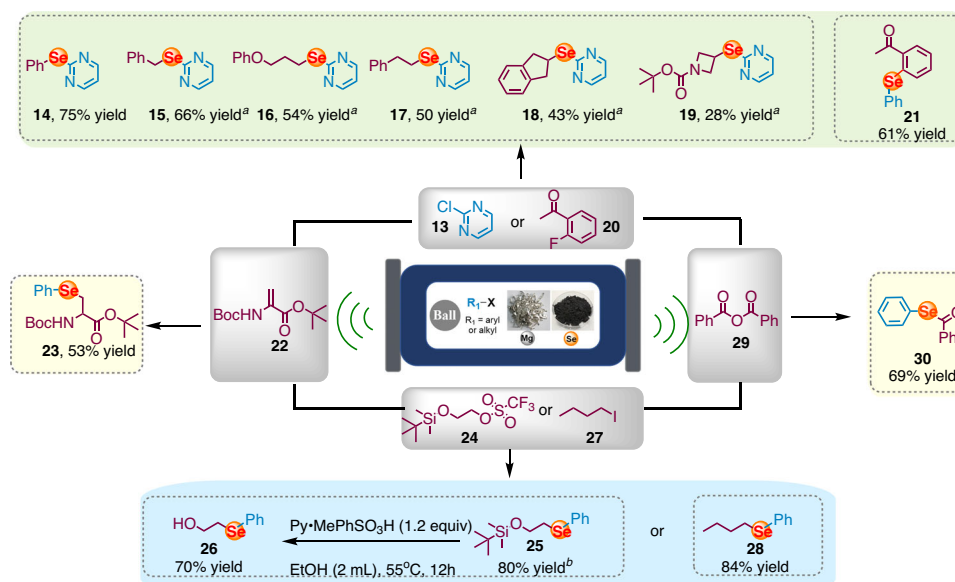
Fig. 3 | Substrate scope for the synthesis of unsymmetrical monochalcogenides using acrylamides as acceptor. **a** Aryl iodide and alkyl iodide coupling partners; **b** Acrylamide coupling partners; **c** Elemental sulfur; **d** Elemental telluride. Reaction conditions: a stainless-steel milling jar (1.5 mL) and a stainless-steel ball (diameter: 6 mm) were used; isolated yields; $\eta = V$ (liquid; μL) / m (reagents; mg). For details, see the Supplementary Information Condition D. **3a** (0.5 mmol), Mg (5.0 equiv), Se (2.0 equiv), **1w** (2.0 equiv), THF ($\eta = 1.3 \mu\text{L}/\text{mg}$) in stainless-steel milling jar (5.0 mL) with a stainless-steel ball (diameter: 10 mm); **1y** = 6-bromo-1-hexene. Additional Mg (1.0 equiv) was added in the second step; for details, see the Supplementary Information Condition F.

in moderate to good yields (**2ra-2rh** and **2sa-2sh**). Due to the plastic feature, S₈ was generally considered inert against mechanical impact, while most of the kinetic energy deriving from the collisions between the balls and sulfur is consumed its deforming rather than for promoting its reactivity⁶⁹. Although investigation in chalcogenation process via ball-milling strategy is raising considerable concern⁷⁰⁻⁷³, direct construction of carbon-chalcogen bond from chalcogen element is rare. Herein, we report the mechanochemical synthesis of organochalcogenides using elemental chalcogen, which showed significant improvement of conversion compared with solution-based condition (Supplementary Information, Supplementary Table 2 and Table 3). Moreover, with modified procedure (Supplementary Information, Condition C), racemic amino acid derivative (**1p**) containing protonic functionality was also applicable, which showcased the compatibility of our method with protonic functionality, which is challenge in the process for preparing Grignard reagents. Besides, this method was applicable for heterocyclic alkyl iodide (**1q**), providing symmetrical alkyl diselenide **2q** in good yield.

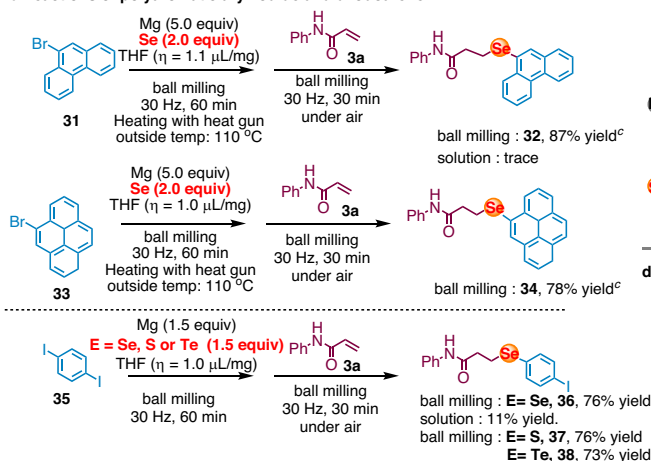
Further, one-pot mechanochemical process was designed to convert elemental selenium directly to unsymmetrical monoselenides (Fig. 3a). We assumed the existence of reaction equilibrium between symmetrical diselenide (**2**) and magnesium-based selenium nucleophiles (**2'**) in the presence of excess amount of magnesium under ball-milling condition, therefore the symmetrical diselenide (**2**) would gradually transform to monoselenides in the presence of electrophile. As expected, when *N*-phenylacrylamide (**3a**) was added in air, the subsequent ball-milling reaction afforded conjugate addition product **4a** in 94% yield (For detailed screening, see the Supplementary Information, Supplementary Table 3). Our protocol was found to be general and robust with remarkable functional group tolerance even in the presence of protonic *NH* functional group of the acrylamides substrates. A broad range of electronic and sterically differentiated substituted iodoarenes as well as heterocycles delivered the corresponding products in excellent yields (**4a-4w**). Alkyl iodide was also competent, the unsymmetrical dialkylselenide (**4x-4z**) was obtained, although elevated temperature was required to achieve satisfactory yield. The methodology is also amenable to the utilization of different acrylamides as acceptors (Fig. 3b). Both electron-donating and electron-withdrawing substituents at *para*- and *meta*-position on the aryl group bound to nitrogen were well tolerated (**5-7**). *N*-alkylacrylamides (**8** and **9**) as well as (*2E*)-*N*-phenyl-butenamide (**10**) were also compatible, although the reactivity is moderate. Moreover, our protocol could be further applied to the facile synthesis of unsymmetrical monosulfides and monotellurides in moderate to good yield (**11a-11n** and **12a-12n**, Fig. 3c and 3d).

Having demonstrated the validity of our method, we next used our solid-state strategy to target other selenation processes that involved alternative electrophilic traps (Fig. 4a). Nucleophilic substitution of 2-chloropyrimidine (**13**) and 2-fluoroacetophenone (**20**) afforded diarylselenoethers (**14** and **21**) efficiently. In addition, alkyl iodides were also compatible, providing versatile alkyl-heteroaryl monoselenides (**15-19**) in good yield. As an alternative, switching the electrophile with alkyl triflate (**24**) and alkyl iodide (**27**) provided corresponding dialkylselenoethers (**26** and **28**) with excellent yield.

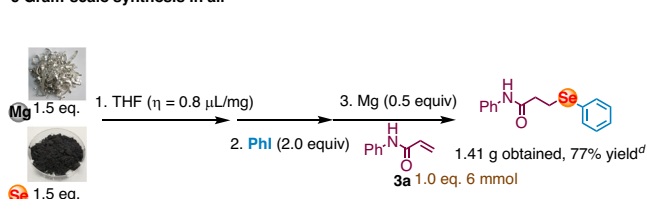
a Versatile electrophiles as acceptors



b Reactions of polyaromatic aryl iodide and diiodoarene



c Gram-scale synthesis in air



d Synthesis of bioactive organoselenium compound

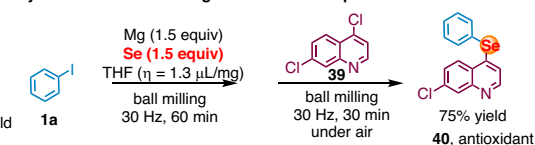


Fig. 4 | Solid-state selenations using challenging substrates, their application in scale-up and bioactive antioxidant synthesis. **a** Versatile electrophiles as acceptors; **b** Reactions of polyaromatic aryl iodide and diiodoarene; **c** Gram-scale synthesis in air; **d** Synthesis of bioactive organoselenium compound. Reaction conditions: a stainless-steel milling jar (1.5 mL) and a stainless-steel ball (diameter: 6 mm) were used; isolated yields. For details, see the Supplementary Information.^a Additional Mg (1.0 equiv) was added in the second step. For details, see Supplementary Information Condition J. ^b **24** (1.0 mmol), Mg (0.5 equiv), Se (0.5 equiv), **1a** (0.5 equiv), LiCl (0.75 equiv), THF ($\eta = 0.8 \mu\text{L}/\text{mg}$) in stainless-steel milling jar (5 mL)

with a stainless-steel ball (diameter: 10 mm). For details, see Supplementary Information Condition I. ^c **3a** (0.5 mmol), Mg (5.0 equiv), Se (2.0 equiv), **31/33** (2.0 equiv), THF ($\eta = 1.1 \mu\text{L}/\text{mg}$) in stainless-steel milling jar (5 mL) with a stainless-steel ball (diameter: 10 mm). For details, see Supplementary Information Condition G. ^d **3a** (6 mmol), THF ($\eta = 0.8 \mu\text{L}/\text{mg}$) in stainless-steel milling jar (10 mL) with a stainless-steel ball (diameter: 15 mm). For details, see the Supplementary Information Methods' synthesis of unsymmetrical monochalcogenides with gram-scale reaction.

Conjugate addition reaction using α , β -unsaturated amino acid derivative (**22**) as electrophile provided selenium-containing amino acid in good yield (**23**). The protocol could also be applied to the facile construction of selenoesters, a type of important synthetic intermediates and widely applied to the synthesis of important bioactive compounds^{74–78}. Using anhydride (**29**) as trapping reagent, corresponding selenol ester (**30**) was synthesized with significantly improved step and atomic efficiency compared with other strategies^{79–82}.

Large polyaromatic aryl halides (**31** and **33**) were submitted to the one-pot selenation sequence using *N*-phenylacrylamide as electrophile. Previous studies have suggested that external heating can improve the mixing efficiency and promote chemical reactions in solid state^{83–85}. To further enhance reactivity, we employed a commercially

available, temperature-controllable heat gun, positioned it directly above the ball-milling jar, with the temperature set at 110 °C (For detailed screening of reaction parameters, see the Supplementary Information, Supplementary Fig. 4.). While solution-based condition failed, our strategy performed effectively under the optimized condition, yielding selenation product **32** and **34** in good yields. In the case of diiodoarene (**35**), monoselective selenation in solid state afforded **36** in good yield and excellent selectivity, while solution-based condition provided complex crude mixture with only 10% yield of product. Furthermore, this reaction offers the advantage of yielding monochalcogenides with good yields and selectivity (**37** and **38**). The robust nature of the current process was further highlighted by scaled-up experiment using bench THF as LAG in air (Fig. 4c) with slightly modified procedure, which successfully produced desired product

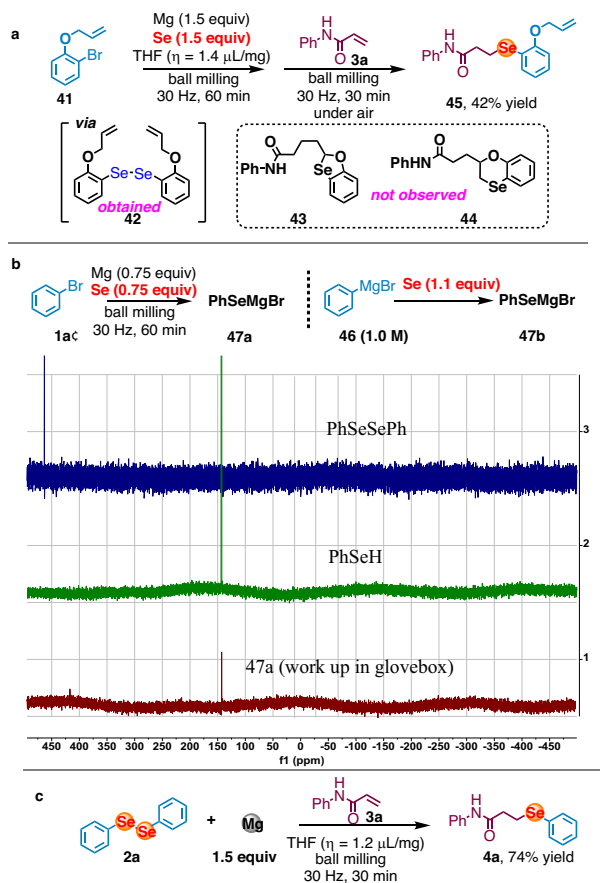


Fig. 5 | Mechanistic Insights. **a** Radical cyclization experiment. **b** NMR of intermediate. **c** Cleavage of Se-Se bond using magnesium.

without using anhydrous solvent as well as tedious schlenk technique. Moreover, our method could also be applied to the facile synthesis of bioactive compounds. Starting from 4,7-dichloroquinoline (**39**), **40** with potential antioxidant and anticholinesterase activities could be efficiently synthesized regioselectively in one-pot with 75% yield⁸⁶.

Preliminary mechanistic experiments were carried out to shed light on the ball-milling-enabled one-pot selenation process. Substrate with radical cyclization potential (**41**) was evaluated and only linear symmetrical diselenide intermediate (**42**) and unsymmetrical monoselenide (**45**) was obtained exclusively without observation of any cyclized byproduct (**43** or **44**), which indicated the reaction may proceed via two electron 1,4- nucleophilic addition pathway while not radical pathway initiated by one electron reduction of diselenide from magnesium under ball-milling condition⁸⁷ (Fig. 5a). Conducting standard reaction under argon protection and subsequently performing the work-up via short column filtration in a glove box resulted in the exclusive formation of benzeneselenol (as depicted in Fig. 5b, **47a**). In contrast, in previous experiments depicted in Fig. 2, when the work-up was conducted in the presence of air, it exclusively led to the formation of the symmetrical diselenide. This outcome strongly indicates that the Se-Se bond forming process occurs via air oxidation. Moreover, in the presence of magnesium, diphenyl diselenide (**2a**) could be converted to corresponding product **4a** efficiently within 30 min (Fig. 5c). It is worth noting that the cleavage of Se-Se bond using magnesium alone was previously regarded as a challenging task⁸⁸. This observation indicates that symmetrical diselenides, which are generated in situ upon exposure to air, can be efficiently converted to selenium nucleophiles in the presence of magnesium under ball-milling condition. Subsequent exposure to electrophiles led to the formation of unsymmetrical monoselenide in good yields.

To confirm the generation of magnesium-based selenium nucleophiles under ball-milling conditions, we utilized Near-edge X-ray absorption fine structure (NEXAFS) spectroscopy. NEXAFS measurements were conducted at BL08U1A beamline of Shanghai Synchrotron Radiation Facility (SSRF in China) using magnesium-based selenium nucleophiles **47a** which were prepared through ball milling and then transferred into the soft X-ray optics under an argon atmosphere. The formation of the divalent cationic Mg^{2+} species was unequivocally confirmed through the high-energy shift of the Mg K-absorption edge (1317.0 eV) in comparison to the Mg^0 edge (1315.0 eV) of a standard magnesium flake⁸⁹.

(Figure 6a). The high resemblance of the NEXAFS spectra at Mg-K, C-K Se-L₃ edges between the mechanochemically-prepared **47a** and PhSeMgBr prepared in solution **47b**⁹⁰ (Fig. 5b) supports the formation of similar magnesium-based organoselenium species with carbon-selenium bonds under both ball-milling and solution conditions in THF (Fig. 6a-c). The presence of carbon-selenium bond, arising from the transformation of the C-Br bond in the starting bromobenzene, was supported by the intense $1s-\pi^*$ transition peaks at approximately 284.0 and 286.2 eV in the C-K NEXAFS spectra (Fig. 6b)⁹¹. Additionally, the formation of the monovalent anionic Se⁻ species was conclusively confirmed through the low-energy shift of the Se L₃-edge absorption peak (1445.3 eV) in **47a** relative to the Se⁰ peak (1446.0 eV) in standard selenium powder (Fig. 6c)⁹². The remarkable similarity of Se L₃-edge, Mg K-edge and C K-edge NEXAFS spectra of mechanochemically-prepared **47a** to those of PhSeMgBr (**47b**) prepared in solution (Fig. 6a-c) further supports the formation of similar organoselenium species with carbon-selenium bonds under both ball-milling and solution conditions in THF⁶⁰.

Discussion

In summary, we developed the ball-milling-enabled C-Se bond formation from readily accessible organic halides, magnesium metal and elemental selenium. The reaction features a wide substrate scope, tolerating protonic, steric and electronic different functionalities. The simple and efficient one-pot operation afforded a wide range of symmetrical diselenides and unsymmetrical monoselenides, respectively, whose formation would otherwise require transition metal catalysts, large excess of hazardous organic solvents and extensive heating. The synthetic potential of the solid-state selenation protocols was showcased through the facile access to a selenium-containing biologically important molecule (**40**). We envisage that our solid-state one-pot selenation strategy will serve as a launchpad for the invention of chalcogenation processes and related projects are ongoing in our laboratory.

Methods

General procedure for the synthesis of symmetrical dichalcogenides

Mg turnings (0.2 mmol, 1.0 equiv, 4.8 mg) and Se powder (0.2 mmol, 1.0 equiv, 16.0 mg) were placed in a jar (stainless-steel; 1.5 mL) with a ball stainless-steel; 6 mm, diameter) in argon. An organic halide **1** (0.2 mmol, 1.0 equiv), LiCl (0.3 mmol, 1.5 equiv, 12.7 mg) and THF (1.1-1.6 μ L/mg) were added to the jar using a syringe. After the jar was closed, the jar was placed in a ball mill (Retsch MM 400, 15-30 min, 30 Hz). After grinding for 15-30 min, the mixture was eluted from silica gel with EA (ethyl acetate), the solvent was removed by vacuum distillation, and the pure product was obtained by rapid column chromatography (SiO₂, Hexane).

General procedure for the synthesis of unsymmetrical monochalcogenides

Mg turnings (0.3 mmol, 1.5 equiv, 7.2 mg) and Se powder (0.3 mmol, 1.5 equiv, 24.0 mg) were placed in a jar (stainless-steel; 1.5 mL) with a ball (stainless-steel; 6 mm, diameter) in argon. An organic halide **1**

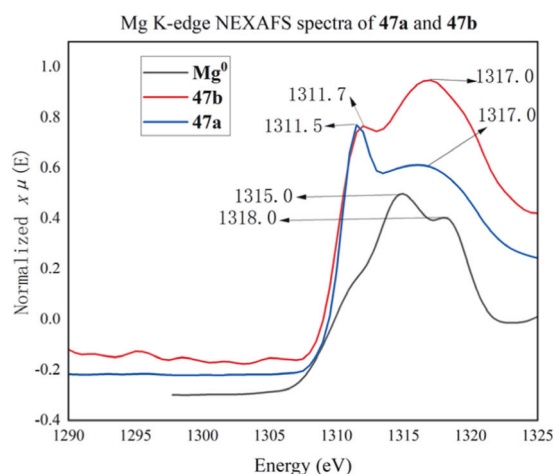
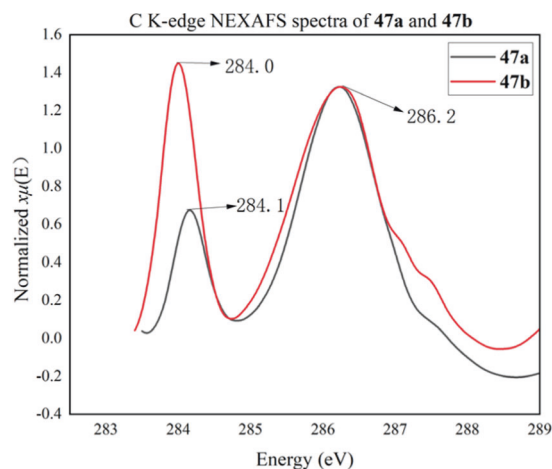
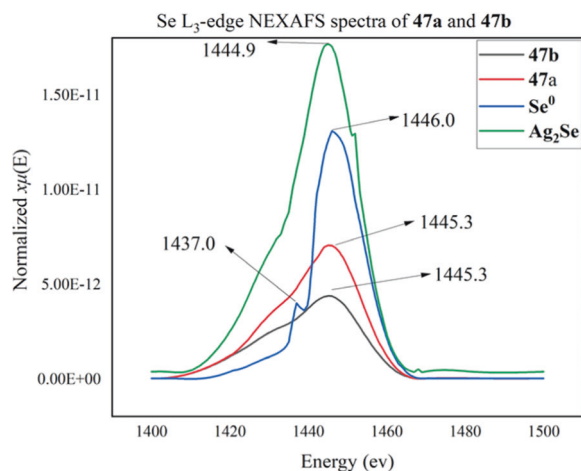
a Mg K-edge NEXAFS spectra of 47a and 47b**b C K-edge NEXAFS spectra of 47a and 47b****c Se L₃-edge NEXAFS spectra of 47a and 47b**

Fig. 6 | NEXAFS analysis of a magnesium-based selenium nucleophiles under mechanochemical conditions. **a** Mg K-edge NEXAFS spectra of mechanochemically prepared **47a**, **47b**, and a magnesium flake of Mg^0 standard. **b** C K-edge NEXAFS spectra of mechanochemically prepared **47a**, **47b**. **c** Se L₃-edge NEXAFS spectra of mechanochemically prepared **47a**, **47b** and selenium flake of Se^0 and Ag_2Se standard.

(0.4 mmol, 2.0 equiv) and THF (0.8–1.4 $\mu\text{L}/\text{mg}$) were added to the jar using a syringe. After the jar was closed, the jar was placed in a ball mill (Retsch MM 400, 60 min, 30 Hz). After grinding for 60 min, the jar was opened in air and charged with an electrophile **3** (0.20 mmol, 29.4 mg). The jar was then closed without purging with inert gas, and was placed in the ball mill (Retsch MM 400, 30–60 min, 30 Hz). After grinding for 30–60 min, the mixture was eluted from silica gel with EA (ethyl acetate), the solvent was removed by vacuum distillation, and the pure product was obtained by rapid column chromatography (SiO_2 , petroleum ether/ethyl acetate, 10:1–5:1).

Data availability

For full characterization data including NMR/IR/HR-MS spectra of the new compounds and experimental details, see the Supplementary Material. All relevant data underlying the results of this study are available from the corresponding authors upon request.

References

- Reich, H. J. & Hondal, R. J. Why nature chose selenium. *ACS Chem. Biol.* **11**, 821–841 (2016).
- Hou, W. et al. Selenium as an emerging versatile player in heterocycles and natural products modification. *Drug Discov. Today* **27**, 2268–2277 (2022).
- Radomska, D., Czarnomysy, R., Radomski, D. & Bielawski, K. Selenium compounds as novel potential anticancer agents. *Int. J. Mol. Sci.* **22**, 1009 (2021).
- Ali, W., Benedetti, R., Handzlik, J., Zwergel, C. & Battistelli, C. The innovative potential of selenium-containing agents for fighting cancer and viral infections. *Drug Discov. Today* **26**, 256–263 (2021).
- Wagner, M. S. et al. Revitalizing the AZT through of the selenium: an approach in human triple negative breast cancer cell line. *Front. Oncol.* **8**, 525 (2018).
- Domingues, M. et al. Selanylimidazopyridine abolishes inflammation- and stress-induced depressive-like behaviors by modulating the oxido-nitrosative system. *Eur. J. Pharmacol.* **914**, 174570 (2022).
- Liao, L.-H. & Zhao, X.-D. Modern organoselenium catalysis: opportunities and challenges. *Synlett* **32**, 1262–1268 (2021).
- Shao, L.-X., Li, Y.-M., Lu, J.-M. & Jiang, X.-F. Recent progress in selenium-catalyzed organic reactions. *Org. Chem. Front.* **6**, 2999–3041 (2019).
- Mumford, E. M., Hemric, B. N. & Denmark, S. E. Catalytic, enantioselective syn-oxyamination of alkenes. *J. Am. Chem. Soc.* **143**, 13408–13417 (2021).
- Wang, W. et al. Dual chalcogen–chalcogen bonding catalysis. *J. Am. Chem. Soc.* **142**, 3117–3124 (2020).
- Teh, W. P., Obenschain, D. C., Black, B. M. & Michael, F. E. Catalytic metal-free allylic C–H amination of terpenoids. *J. Am. Chem. Soc.* **142**, 16716–16722 (2020).
- Guo, R.-Z., Liu, Z.-Q. & Zhao, X.-D. Efficient synthesis of P–P-Chirogenic compounds enabled by chiral selenide-catalyzed enantioselective electrophilic aromatic halogenation. *CCS. Chemistry* **3**, 2617–2628 (2021).
- Liu, X., Liang, Y.-Y., Ji, J.-Y., Luo, J. & Zhao, X.-D. Chiral selenide-catalyzed enantioselective allylic reaction and intermolecular difunctionalization of alkenes: efficient construction of C–SCF₃ stereogenic molecules. *J. Am. Chem. Soc.* **140**, 4782–4786 (2018).
- He, X.-X., Wang, X.-Y., Tse, Y.-L.-S., Ke, Z.-H. & Yeung, Y.-Y. Applications of selenium cations as Lewis acids in organocatalytic reactions. *Angew. Chem. Int. Ed.* **57**, 12869–12873 (2018).
- Liao, L.-H., Guo, R. Z. & Zhao, X.-D. Organoselenium-catalyzed regioselective C–H pyridination of 1,3-dienes and alkenes. *Angew. Chem. Int. Ed.* **56**, 3201–3205 (2017).

16. Kawamata, Y., Hashimoto, T. & Maruoka, K. A chiral electrophilic selenium catalyst for highly enantioselective oxidative cyclization. *J. Am. Chem. Soc.* **138**, 5206–5209 (2016).
17. Denmark, S. E. & Chi, H. M. Lewis base catalyzed, enantioselective, intramolecular sulfenoamination of olefins. *J. Am. Chem. Soc.* **136**, 8915–8918 (2014).
18. Denmark, S. E., Hartmann, E., Kornfilt, D. J. P. & Wang, H. Mechanistic, crystallographic, and computational studies on the catalytic, enantioselective sulfenofunctionalization of alkenes. *Nat. Chem.* **6**, 1056–1064 (2014).
19. Hoover, G. C. & Seferos, D. S. Photoactivity and optical applications of organic materials containing selenium and tellurium. *Chem. Sci.* **10**, 9182–9188 (2019).
20. Xia, J.-H., Li, T.-Y., Lu, C.-J. & Xu, H.-P. Selenium-containing polymers: perspectives toward diverse applications in both adaptive and biomedical materials. *Macromolecules* **51**, 7435–7455 (2018).
21. Reich, H. J. Functional group manipulation using organoselenium reagents. *Acc. Chem. Res.* **12**, 22–30 (1979).
22. Kalaramna, P. & Goswami, A. Transition-metal-free HFIP-mediated organo chalcogenylation of arenes/indoles with thio-/selenocyanates. *J. Org. Chem.* **86**, 9317–9327 (2021).
23. Nicolaou, K. C., Petasis, N. A. & Claremon, D. A. *N*-phenylselenophthalimide (NPSF): a valuable selenenylating agent. *Tetrahedron* **41**, 4835–4841 (1985).
24. Sonawane, A. D., Sonawane, R. A., Ninomiya, M. & Koketsu, M. Diorganyl diselenides: a powerful tool for the construction of selenium containing scaffolds. *Dalton Trans.* **50**, 12764–12790 (2021).
25. Ivanova, A. & Arsenyan, P. Rise of diselenides: recent advances in the synthesis of heteroarylselenides. *Coord. Chem. Rev.* **370**, 55–68 (2018).
26. Slocumb, H. S., Nie, S.-Z., Dong, V. M. & Yang, X.-H. Enantioselective selenolene using Rh-hydride catalysis. *J. Am. Chem. Soc.* **144**, 18246–18250 (2022).
27. Xu, H.-T. et al. A chemistry for incorporation of selenium into DNA-encoded libraries. *Angew. Chem. Int. Ed.* **59**, 13273–13280 (2020).
28. Hu, D.-H., Liu, M.-C., Wu, H.-Y., Gao, W.-X. & Wu, G. Copper-catalyzed diarylation of Se with aryl iodides and heterocycles. *Org. Chem. Front.* **5**, 1352–1355 (2018).
29. Wu, S., Shi, J. & Zhang, C.-P. Cu-mediated arylselenylation of aryl halides with trifluoromethyl aryl selenonium ylides. *Org. Biomol. Chem.* **17**, 7468–7473 (2019).
30. Zhang, Q.-B. et al. Visible-light-mediated aerobic selenation of (hetero)arenes with diselenides. *Green. Chem.* **19**, 5559–5563 (2017).
31. Zhou, J.-L. et al. Visible light-induced cascade cyclization of 3-aminoindazoles, ynals, and chalcogens: access to chalcogen-containing pyrimido[1,2-*b*]-indazoles. *Org. Lett.* **23**, 2754–2759 (2021).
32. Wang, R.-Z. et al. Metal-free photochemical C–Se cross-coupling of aryl halides with diselenides. *Adv. Synth. Catal.* **364**, 1607–1612 (2022).
33. Chen, Z.-Y. et al. Electrochemical Mn-promoted radical selenylation of boronic acids with diselenide reagents. *Org. Lett.* **24**, 3307–3312 (2022).
34. Dutta, S., Saha, A. & Ranu, B. C. Solvent free synthesis of organoselenides under green conditions. *N. J. Chem.* **46**, 21489–21518 (2022).
35. Chatterjee, T. & Ranu, B. C. Synthesis of organosulfur and related heterocycles under mechanochemical conditions. *J. Org. Chem.* **86**, 13895–13910 (2021).
36. Santi, C. et al. Water and aqueous mixtures as convenient alternative media for organoselenium chemistry. *Molecules* **21**, 1482–1498 (2016).
37. Ma, Y.-T., Liu, M.-C., Zhou, Y.-B. & Wu, H.-Y. Synthesis of organoselenium compounds with elemental selenium. *Adv. Synth. Catal.* **363**, 5386–5406 (2021).
38. Stolle, A., Szuppa, T., Leonhardt, S. E. S. & Ondruschka, B. Ball milling in organic synthesis: solutions and challenges. *Chem. Soc. Rev.* **40**, 2317–2329 (2011).
39. James, S. L. et al. Mechanochemistry: opportunities for new and cleaner synthesis. *Chem. Soc. Rev.* **41**, 413–447 (2012).
40. Wang, G.-W. Mechanochemical organic synthesis. *Chem. Soc. Rev.* **42**, 7668–7700 (2013).
41. Howard, J. L., Cao, Q. & Browne, D. L. Mechanochemistry as an emerging tool for molecular synthesis: what can it offer? *Chem. Sci.* **9**, 3080–3094 (2018).
42. Andersen, J. & Mack, J. Mechanochemistry and organic synthesis: from mystical to practical. *Green. Chem.* **20**, 1435–1443 (2018).
43. Bolm, C. & Hernández, J. G. Mechanochemistry of gaseous reactants. *Angew. Chem. Int. Ed.* **58**, 3285–3299 (2019).
44. Tan, D. & García, F. Main group mechanochemistry: from curiosity to established protocols. *Chem. Soc. Rev.* **48**, 2274–2292 (2019).
45. Porcheddu, A., Colacino, E., De Luca, L. & Delogu, F. Metal-mediated and metal-catalyzed reactions under mechanochemical conditions. *ACS Catal.* **10**, 8344–8394 (2020).
46. Kubota, K. & Ito, H. Mechanochemical cross-coupling reactions. *Trends Chem.* **2**, 1066–1081 (2020).
47. Mateti, S. et al. Mechanochemistry: a force in disguise and conditional effects towards chemical reactions. *Chem. Commun.* **57**, 1080–1092 (2021).
48. Harrowfield, J. M., Hart, R. J. & Whitaker, C. R. Magnesium and aromatics: mechanically-induced grignard and McMurry Reactions. *Aust. J. Chem.* **54**, 423–425 (2001).
49. Birke, V., Schütt, C., Burmeier, H. & Ruck, W. Defined mechanochemical reductive dechlorination of 1,3,5-trichlorobenzene at room temperature in a ball mill. *Fresenius Environ. Bull.* **20**, 2794–2805 (2011).
50. Zhdanko, A., Ströbele, M. & Maier, M. E. Coordination chemistry of Gold catalysts in solution: a detailed NMR study. *Chem. -Eur. J.* **18**, 14732–14744 (2012).
51. Egbert, J. D., Slawin, A. M. Z. & Nolan, S. P. Synthesis of *N*-heterocyclic carbene gold complexes using solution-phase and solid-state protocols. *Organometallics* **32**, 2271–2274 (2013).
52. Hernández, J. G., Butler, I. S. & Friščić, T. Multi-step and multi-component organometallic synthesis in one pot using orthogonal mechanochemical reactions. *Chem. Sci.* **5**, 3576–3582 (2014).
53. Speight, I. R. & Hanusa, T. P. Exploration of mechanochemical activation in solid-state fluoro-Grignard reactions. *Molecules* **25**, 570 (2020).
54. Cao, Q., Stark, R. T., Fallis, I. A. & Browne, D. L. A ball-milling-enabled reformatsky reaction. *ChemSusChem* **12**, 2554–2557 (2019).
55. Yin, J.-X., Stark, R. T., Fallis, I. A. & Browne, D. L. A mechanochemical zinc-mediated barbier-type allylation reaction under ball-milling conditions. *J. Org. Chem.* **85**, 2347–2354 (2020).
56. Gao, P., Jiang, J.-L., Maeda, S., Kubota, K. & Ito, H. Mechanochemically generated calcium-based heavy grignard reagents and their application to carbon–carbon bond-forming reactions. *Angew. Chem. Int. Ed.* **61**, e202207118 (2022).
57. Gao, Y.-P., Kubota, K. & Ito, H. Mechanochemical approach for air-tolerant and extremely fast lithium-based birch reductions in minutes. *Angew. Chem. Int. Ed.* **62**, e202217723 (2023).
58. Takahashi, R., Gao, P., Kubota, K. & Ito, H. Mechanochemical protocol facilitates the generation of arylmanganese nucleophiles from unactivated manganese metal. *Chem. Sci.* **14**, 499–505 (2023).
59. Jones, A. C., Leitch, J. A., Raby-Buck, S. E. & Browne, D. L. Mechanochemical techniques for the activation and use of zero-valent metals in synthesis. *Nat. Synth.* **1**, 763–775 (2022).
60. Takahashi, R. et al. Mechanochemical synthesis of magnesium-based carbon nucleophiles in air and their use in organic synthesis. *Nat. Commun.* **12**, 6691 (2021).

61. Pfenning, V. S., Vilella, R. C., Nikodemus, J. & Bolm, C. Mechanochemical grignard reactions with gaseous CO₂ and sodium methyl carbonat. *Angew. Chem. Int. Ed.* **61**, e02116514 (2022).
62. Gao, F. et al. A novel regioselective reaction of styrene with magnesium organoselenolates to afford unsymmetrical selenides catalyzed by CuI and L-proline. *Tetrahedron Lett.* **53**, 5688–5690 (2012).
63. Clarebeau, M. et al. Synthesis of selenoacetals. *Tetrahedron* **41**, 4793–4812 (1985).
64. Gerdt, P. & Studer, A. Alternating terpolymers through cyclo-polymerization and subsequent orthogonal functionalization. *Angew. Chem. Int. Ed.* **61**, e202206964 (2022).
65. Li, Y.-M. et al. A highly efficient method for the copper-catalyzed selective synthesis of diaryl chalcogenides from easily available chalcogen sources. *Eur. J. Org. Chem.* **2011**, 7331–7338 (2011).
66. Taniguchi, N. Copper-catalyzed chalcogenation of aryl iodides via reduction of chalcogen elements by aluminum or magnesium. *Tetrahedron* **68**, 10510–10515 (2012).
67. Li, Z.-K. et al. Synthesis of disulfides and diselenides by copper-catalyzed coupling reactions in water. *Org. Biomol. Chem.* **11**, 2943–2946 (2013).
68. Soleiman-Beigi, M., Yavari, I. & Sadeghizadeh, F. The direct synthesis of symmetrical disulfides and diselenides by metal-organic framework MOF-199 as an efficient heterogeneous catalyst. *RSC Adv.* **5**, 87564–87570 (2015).
69. Heinicke, G., Riedel, R. & Harenz, H. Oxidation reactions by impact treatment. *Ztschr. Phys. Chem.* **227**, 62–80 (1964).
70. Kumar, R. et al. Synthesis of phosphine chalcogenides under solvent-free conditions using a rotary ball mill. *Eur. J. Inorg. Chem.* **8**, 1028–1037 (2018).
71. Sim, Y., Tan, D., Ganguly, R., Li, Y.-X. & García, F. Orthogonality in main group compounds: a direct one-step synthesis of air- and moisture-stable cyclophosphazanes by mechanochemistry. *ChemComm* **54**, 6800–6803 (2018).
72. Chua, C. K., Sofer, Z., Khezri, B., Webster, R. D. & Pumera, M. Ball-milled sulfur-doped graphene materials contain metallic impurities originating from ball-milling apparatus: their influence on the catalytic properties. *Phys. Chem. Chem. Phys.* **18**, 17875–17880 (2016).
73. Geng, X.-Z. et al. Effect of the mechanochemical process on the stability of Mercury in simulated fly ash, part 2: sulfur additive. *Ind. Eng. Chem. Res.* **60**, 15115–15124 (2021).
74. Bannasar, M. L., Roca, T. & Ferrando, F. A new radical-based route to calothrixin B. *Org. Lett.* **8**, 561–564 (2006).
75. McGarvey, G. J., Williams, J. M., Hiner, R. N., Matsubara, Y. & Oh, T. L-aspartic acid in acyclic stereoselective synthesis. synthetic studies on amphotericin B. *J. Am. Chem. Soc.* **108**, 4943–4952 (1986).
76. Takei, T., Andoh, T., Takao, T. & Hojo, H. One-Pot four-segment ligation using seleno- and thioesters: synthesis of superoxide dismutase. *Angew. Chem. Int. Ed.* **56**, 15708–15711 (2017).
77. Barbosa, F. A. R., Canto, R. F. S., Saba, S., Rafique, J. & Braga, A. L. Synthesis and evaluation of dihydropyrimidinone-derived selenoesters as multi-targeted directed compounds against Alzheimer's disease. *Biorg. Med. Chem.* **24**, 5762–5770 (2016).
78. Domínguez-Álvarez, E. et al. Synthesis and antiproliferative activity of novel selenoester derivatives. *Eur. J. Med. Chem.* **73**, 153–166 (2014).
79. Andreadou, I., Menge, W. M. P. B., Commandeur, J. N. M., Worthington, E. A. & Vermeulen, N. P. E. Synthesis of novel Se-substituted selenocysteine derivatives as potential kidney selective prodrugs of biologically active selenol compounds: evaluation of kinetics of β-elimination reactions in rat renal cytosol. *J. Med. Chem.* **39**, 2040–2046 (1996).
80. Temperini, A., Piazzolla, F., Minuti, L., Curini, M. & Siciliano, C. General, mild, and metal-free synthesis of phenyl selenoesters from anhydrides and their use in peptide synthesis. *J. Org. Chem.* **82**, 4588–4603 (2017).
81. Baldassari, L. L. et al. Redox-neutral synthesis of selenoesters by oxyarylation of selenoalkynes under mild conditions. *Org. Lett.* **20**, 5881–5885 (2018).
82. de Oliveira, A. J. et al. Synthesis of selenol esters via the reaction of acyl chlorides with diselenides in the presence of Zn dust catalyzed by CoCl₂·6H₂O. *Tetrahedron Lett.* **80**, 153317 (2021).
83. Yong, T., Bâti, G., García, F. & Stuparu, M. C. Mechanochemical transformation of planar polyarenes to curved fused-ring systems. *Nat. Commun.* **12**, 5187 (2021).
84. Martinez, V., Stolar, T., Karadeniz, B., Brekalo, I. & Užarević, K. Advancing mechanochemical synthesis by combining milling with different energy sources. *Nat. Rev. Chem.* **7**, 51–65 (2023).
85. Bâti, G. et al. Mechanochemical synthesis of corannulene-based curved nanographenes. *Angew. Chem. Int. Ed.* **59**, 21620–21626 (2020).
86. Duarte, L. F. B. et al. Organoselenium compounds from purines: synthesis of 6-arylselanyl purines with antioxidant and anticholinesterase activities and memory improvement effect. *Biorg. Med. Chem.* **25**, 6718–6723 (2017).
87. Wu, C. et al. Mechanochemical Magnesium-Mediated Minisci C–H Alkylation of Pyrimidines with Alkyl Bromides and Chlorides. *Org. Lett.* **23**, 6423–6428 (2021).
88. Taniguchi, N. & Onami, T. Magnesium-induced copper-catalyzed synthesis of unsymmetrical diaryl chalcogenide compounds from aryl iodide via cleavage of the Se–Se or S–S Bond. *J. Org. Chem.* **69**, 915–920 (2004).
89. Witte, K. et al. NEXAFS spectroscopy of chlorophyll a in solution. *J. Phys. Chem. B.* **120**, 11619–11627 (2016).
90. Li, Y.-Y. et al. Degradable Selenium-containing polymers for low cytotoxic antibacterial materials. *ACS Macro Lett.* **11**, 1349–1354 (2022).
91. Cooney, R. R. & Urquhart, S. G. Chemical trends in the near-edge X-ray absorption fine structure of monosubstituted and para-bisubstituted benzenes. *J. Phys. Chem. B.* **108**, 18185–18191 (2004).
92. Derfus, A. M., Chan, W. C. W. & Bhatia, S. N. Probing the cytotoxicity of Semiconductor quantum dots. *Nano Lett.* **4**, 11–18 (2004).

Acknowledgements

We thank the High-Level Introduction Plan of Shaanxi Province (71240000000111, X. W.), Natural Science Foundation of Shaanxi Province (2022JM-085, X. W.; 2022JQ-121, C. P.), the start-up funds from Xi'an Jiaotong University (X. W.), National Natural Science Foundation of China (22101224, C. F.), the China Postdoctoral Science Foundation (2021M692544, C. F.), the Fundamental Research Funds for the Central Universities (xzy012021049, C. F.) and Young Talent Fund of Xi'an Association for Science and Technology (095920221321, C. F.). We thank Dr. C. Feng and Dr. G. Chang from the Instrument Analysis Center of XJTU for assistance with NMR analysis. We are grateful to Prof. Rui Shang at the University of Tokyo and Prof. Yohei Shimizu at Hokkaido University for the helpful discussion. We also thank BL08U1A beamline of Shanghai Synchrotron Radiation Facility (SSRF) for providing beamtime.

Author contributions

S. C., C. P. and X. W. conceived the study and designed the experiments. S. C., M. P., J. W., Y. Z. and Z. X. performed the experiments, mechanistic studies, and analyzed the data. J. Z., Jiyou Li, Junliang Lu, C. P. and X. W. directed the project. C. F. and Z. X. made contributions during the revision. C. P., C. F. and X. W. wrote the manuscript with input from all the other authors. All authors discussed the results and the manuscript.

Competing interests

The authors declare no competing interests.

Additional information

Supplementary information The online version contains supplementary material available at <https://doi.org/10.1038/s41467-024-44891-2>.

Correspondence and requests for materials should be addressed to Cheng Peng or Xiaofeng Wei.

Peer review information *Nature Communications* thanks the anonymous reviewers for their contribution to the peer review of this work. A peer review file is available.

Reprints and permissions information is available at <http://www.nature.com/reprints>

Publisher's note Springer Nature remains neutral with regard to jurisdictional claims in published maps and institutional affiliations.

Open Access This article is licensed under a Creative Commons Attribution 4.0 International License, which permits use, sharing, adaptation, distribution and reproduction in any medium or format, as long as you give appropriate credit to the original author(s) and the source, provide a link to the Creative Commons licence, and indicate if changes were made. The images or other third party material in this article are included in the article's Creative Commons licence, unless indicated otherwise in a credit line to the material. If material is not included in the article's Creative Commons licence and your intended use is not permitted by statutory regulation or exceeds the permitted use, you will need to obtain permission directly from the copyright holder. To view a copy of this licence, visit <http://creativecommons.org/licenses/by/4.0/>.

© The Author(s) 2024